© 2018. Published by The Company of Biologists Ltd | Development (2018) 145, dev152868. doi:10.1242/dev.152868

RESEARCH ARTICLE

H2A.Z promotes the transcription of *MIR156A* and *MIR156C* in *Arabidopsis* by facilitating the deposition of H3K4me3

Mingli Xu, Aaron R. Leichty, Tieqiang Hu and R. Scott Poethig*

ABSTRACT

Vegetative phase change in *Arabidopsis thaliana* is mediated by a decrease in the level of *MIR156A* and *MIR156C*, resulting in an increase in the expression of their targets, SQUAMOSA PROMOTER BINDING PROTEIN-LIKE (SPL) genes. Changes in chromatin structure are required for the downregulation of *MIR156A* and *MIR156C*, but whether chromatin structure contributes to their initial elevated expression is unknown. We found that mutations in components of the SWR1 complex (*ARP6*, *SEF*) and in genes encoding H2A.Z (*HTA9* and *HTA11*) reduce the expression of *MIR156A* and *MIR156C*, and accelerate vegetative phase change, indicating that H2A.Z promotes juvenile vegetative identity. However, *arp6* and *sef* did not accelerate the temporal decline in miR156, and the downregulation of *MIR156A* and *MIR156C* was not accompanied by significant change in the level of H2A.Z at these loci. We conclude that H2A.Z contributes to the high expression of *MIR156A*/*MIR156C* early in shoot development, but does not regulate the timing of vegetative phase change. Our results also suggest that H2A.Z promotes the expression of *MIR156A*/*MIR156C* by facilitating the deposition of H3K4me3, rather than by decreasing nucleosome occupancy.

KEY WORDS: Vegetative phase change, miR156, H2A.Z

INTRODUCTION

Shoot development in higher plants consists of a juvenile vegetative phase, an adult vegetative phase and a reproductive phase, which differ in many morphological and physiological traits (Poethig, 2003). The transition from the juvenile to the adult phase of vegetative development is regulated by an increase in the expression of squamosa promoter binding protein (SBP) genes, which is mediated by a decrease in the level of two miRNAs – miR156 and miR157 – that repress these genes. To understand the mechanism of vegetative phase change, it is therefore important to determine how the abundance of miR156 and miR157 is regulated.

miR156 is encoded by eight genes in *Arabidopsis*, two of which, *MIR156A* and *MIR156C*, produce the majority of the mature miR156 transcript and are particularly important for vegetative phase change (Yang et al., 2013; Yu et al., 2013). There is increasing evidence that epigenetic factors play important roles in the regulation of these genes. In particular, the downregulation of *MIR156A* and *MIR156C* during vegetative phase change is associated with a decrease in active histone modification, histone 3 lysine 27 acetylation (H3K27ac), and with an increase in the repressive histone modification, histone 3 lysine 27 trimethylation (H3K27me3), and requires this latter modification (Picó et al., 2015; Xu et al., 2016a). In contrast, the transcription of *MIR156A* is promoted by the nucleosome remodeler, BRAHMA (Xu et al., 2016b), and by the SWR1 complex (SWR1-C), which exchanges the histone variant H2A.Z for H2A (Choi et al., 2016). How these ATP-dependent nucleosome remodelers regulate the expression of *MIR156A* and other genes that encode miR156 is unknown. Here, we explore the mechanism by which SWR1-C regulates the transcription of *MIR156A* and *MIR156C*.

SWR1-C is an evolutionarily conserved multi-protein complex first described in budding yeast (Mizuguchi et al., 2004). Three components of SWR1-C are essential for its function in yeast. The ATPase Swr1 provides the catalytic activity for the complex, and works in association with the accessory proteins Arp6 and Swc6. The orthologue of Swr1 in *Arabidopsis* is PHOTOPERIOD-INDEPENDENT EARLY FLOWERING1 (PIE1); the orthologues of Arp6 and Swc6 are, respectively, ACTIN-RELATED PROTEIN6 (ARP6) and SERRATED LEAVES AND EARLY FLOWERING (SEF). As in yeast, these proteins associate with each other and loss-of-function mutations in any of these proteins cause a significant decrease in H2A.Z (March-Díaz et al., 2007; Wu et al., 2005; Wu et al., 2009b). The phenotype of *pie1*, *arp6* and *sef* closely resembles the phenotype produced by mutations in genes that encode H2A.Z (March-Díaz et al., 2007), strongly suggesting that – as in yeast – the primary function of SWR1-C in *Arabidopsis* is to deposit H2A.Z (Mizuguchi et al., 2004; Wu et al., 2005).

H2A.Z affects many processes in fungi, plants and animals, including gene expression, recombination and DNA repair (Choi et al., 2013; Lu et al., 2009; Morrison and Shen, 2009; Rosa et al., 2013; van Attikum et al., 2007; Xu et al., 2012). In plants, H2A.Z has been implicated in the response to high temperature, the phosphate starvation response, osmotic stress, the immune response, floral induction, female meiosis, recombination, thalianol metabolism and the regulation of microRNA abundance (Choi et al., 2016, 2013; Deal et al., 2005; Kumar and Wigge, 2010; March-Díaz et al., 2008; Nützmann and Osbourn, 2015; Qin et al., 2014; Smith et al., 2010; Sura et al., 2017). The presence of H2A.Z at a locus is typically correlated with a high level of responsiveness to environmental factors (Coleman-Derr and Zilberman, 2012; Sura et al., 2017). Depending on the gene, the presence of H2A.Z may be correlated with an increase or a decrease in gene expression upon induction. This observation supports the conclusion that the presence of H2A.Z increases the susceptibility of a gene to factors that promote or repress transcription, rather than conferring a specific pattern of gene expression.

The mechanism by which H2A.Z affects transcription is still unclear. Some *in vitro* analyses suggest that H2A.Z destabilizes nucleosomes, whereas others indicate that it increases nucleosome stability (Abbott et al., 2001; Bowerman and Wereszczynski, 2016;

Department of Biology, University of Pennsylvania, Philadelphia, PA 19104, USA.

*Author for correspondence (spoethig@sas.upenn.edu)

A.R.L., 0000-0003-1071-7921; R.S.P., 0000-0001-6592-5862

Received 30 March 2017; Accepted 20 December 2017

Development (2018) 145, dev152868. doi:10.1242/dev.152868

Hoch et al., 2007; Hong et al., 2014; Jin and Felsenfeld, 2007; Kruger et al., 1995). Similarly, in *Arabidopsis*, mutations that block the deposition of H2A.Z can either increase (Choi et al., 2016; Nützmann and Osbourn, 2015) or decrease (Kumar and Wigge, 2010) nucleosome occupancy. The possibility that H2A.Z affects transcription by influencing modifications of other histone proteins is suggested by the observation that H2A.Z colocalizes with H3K4me3 near the transcription start site (TSS) of many genes (Choi et al., 2013), and by the observation that the abundance of H3K4me3 at *FLC* is reduced in *arp6* mutants (Martin-Trillo et al., 2006).

A previous study showed that *arp6* reduces the abundance of miR156, in part by reducing the expression of *MIR156A* (Choi et al., 2016). However, the biological significance of this effect is unclear because these investigators also found that *arp6* reduces the expression of *MIR172B*, when the expected effect of a reduction in miR156 is an increase in *MIR172B* expression (Wu et al., 2009a). Whether ARP6 contributes to the downregulation of *MIR156A* during vegetative phase change was not investigated in this study.

To address these issues and explore the mechanism by which H2A.Z regulates gene expression in *Arabidopsis*, we compared the effect of mutations in components of SWR1-C on the expression pattern and the chromatin structure of *MIR156A* and *MIR156C*. We found that H2A.Z contributes to the high expression of *MIR156A* and *MIR156C* early in shoot development, but does not play a major role in their downregulation during vegetative phase change. Our results also suggest that H2A.Z promotes the expression of *MIR156A* and *MIR156C* by promoting the deposition of H3K4me3, rather than through an effect on nucleosome occupancy.

RESULTS

Vegetative phase change is accelerated by mutations in components of SWR1-C

In a screen for mutations that accelerate vegetative phase change, we isolated seven alleles of *EARLY IN SHORT DAYS* (*esd1-3* to *esd1-9*), also known as *ACTIN-RELATED PROTEIN 6* (*ARP6*) (Martin-Trillo et al., 2006). These mutants produce fewer juvenile leaves than normal, and flower early in both long days (LDs) and short days (SDs). The early flowering phenotype of *arp6* mutants is the result of the reduced expression of the floral repressor *FLOWERING LOCUS C* (*FLC*) and of genes in the FLC-related MADS-affecting flowering (MAF) gene family (Choi et al., 2005, 2007; Deal et al., 2005, 2007; Lázaro et al., 2008; Martin-Trillo et al., 2006). However, the mechanism by which *arp6* affects vegetative phase change – which is regulated independently of *FLC* (Willmann and Poethig, 2011) – remains unknown.

ARP6 interacts with SERRATED AND EARLY FLOWERING (SEF) to facilitate the exchange of histone variant H2A.Z for H2A (Choi et al., 2007; March-Díaz et al., 2007). To determine whether ARP6 affects vegetative phase change through its effect on H2A.Z, we compared the vegetative phenotype of *arp6* and *sef* mutants with plants deficient for H2A.Z. In *Arabidopsis*, H2A.Z is encoded by *HTA8*, *HTA9* and *HTA11* (Coleman-Derr and Zilberman, 2012; Redon et al., 2002; Yi et al., 2006). The *hta9 hta11* double mutant is morphologically and physiologically similar to *arp6* mutants (Cheng et al., 2013; Coleman-Derr and Zilberman, 2012; Kumar and Wigge, 2010; March-Díaz et al., 2008), so we focused on this genotype. We compared the phenotype of these mutants with plants doubly mutant for *mir156a-2* and *mir156c-1* to determine the extent to which their vegetative phenotype may be explained by a decrease in the level of miR156. The alleles used for this analysis are null alleles and have been extensively characterized by other investigators (Cheng et al., 2013; Coleman-Derr and Zilberman, 2012; Deal et al., 2005; Kumar and Wigge, 2010; March-Díaz et al., 2008; Yang et al., 2013).

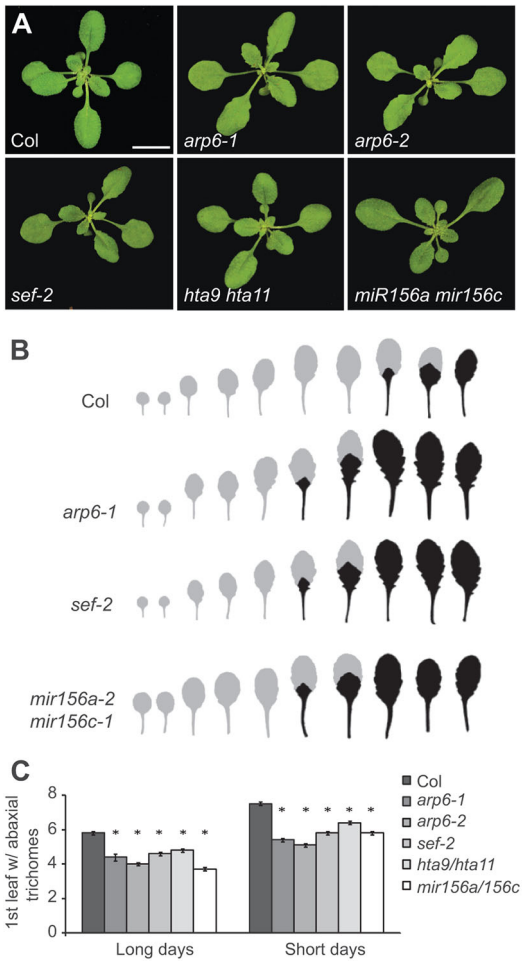

Fig. 1. Vegetative phase change is accelerated by mutations in genes encoding H2A.Z and components of SWR1-C. (A) 17-day-old Col, *arp6-1*, *arp6-2*, *sef-1*, *hta9-1 hta11-2* and *mir156a-2 mir156c-1* mutants grown under long-day (LD) conditions. Scale bar: 1 cm. (B) Fully expanded rosette leaves of Col, *arp6-1, sef-2* and *mir156a-2 mir156c-1*. Gray indicates the absence of abaxial trichomes; black indicates the presence of abaxial trichomes. (C) First leaf with abaxial trichomes in Col, *swr1-c* mutants (*arp6-1, arp6-2, sef-2*), *h2a.z* mutants (*hta9-1 hta11-2*) and the *mir156a mir156c* double mutant under LD and short-day (SD) conditions. *P<0.001, Dunnett's test, n=20-24 for each genotype; data are mean±s.e.m.

In *Arabidopsis*, juvenile rosette leaves are round with smooth margins and do not produce trichomes on their abaxial surface, whereas adult leaves are elongated, have a serrated margin, and produce trichomes on both sides of the leaf. Leaf 3 and leaf 4 of *arp6-1*, *arp6-2*, *sef-2* and *hta9-1 hta11-2* were more elongated and serrated than the corresponding leaves in Col under both long-day (LD) and short-day (SD) conditions (Fig. 1A,B). *arp6-1*, *arp6-2*, *sef-2* and *hta9-1 hta11-2* also accelerated the production of abaxial trichomes (Fig. 1C). In these respects, these mutants were similar to the *mir156a-2 mir156c-1* double mutant (Fig. 1A,B). This result demonstrates that H2A.Z promotes the expression of the juvenile vegetative phase, and suggests that it may do so by promoting the expression of *MIR156A* and/or *MIR156C*.

Development (2018) 145, dev152868. doi:10.1242/dev.152868

ARP6 and SEF promote the juvenile phase by activating the transcription of *MIR156A* and *MIR156C*

To determine whether SWR1-C regulates vegetative phase change by affecting the expression of miR156, we measured the abundance of miR156 in shoot apices of wild-type Col and *arp6*-1 (hereafter *arp6*), and *sef*-2 (hereafter *sef*) mutants grown in short days (SD). Shoot apices were harvested at time points corresponding to the juvenile (L1+), juvenile and transition (L3+, L5+) and adult (L7+) phases of shoot development. The largest leaf primordium in these samples (leaf 1, 3, 5 or 7, respectively) was 2-3 mm. RT-qPCR revealed that *arp6* and *sef* had significantly lower than normal levels of miR156 at the earliest juvenile stage (L1+), but not at later stages of shoot development (Fig. 2A). We then examined the effect of these mutations on the primary transcripts of *MIR156A* (pri-miR156a) and *MIR156C* (pri-miR156c). Both transcripts were present at 59-67% of the wild-type (Col) level in the shoot apex of 1-week-old *arp6* and *sef* seedlings (L1+ stage) (Fig. 2B). This decrease was associated with a 1.3-to 2.1-fold increase in the transcripts of two direct targets of miR156, *SPL9* and *SPL15* (Fig. 2C). To determine whether the effect of *arp6* on *SPL9* expression is attributable to its effect on miR156, we crossed miR156-sensitive (*pSPL9::SPL9-GUS*) and miR156-resistant (*pSPL9::rSPL9-GUS*) reporters into an *arp6* background. *arp6* increased the GUS activity of the miR156-sensitive reporter by twofold, but had no effect on the activity of the miR156-resistant reporter (Fig. 2D,E). This result demonstrates that the effect of *arp6* on *SPL9* requires miR156 activity, and suggests that *arp6* increases the expression of *SPL9* by reducing the abundant miR156, rather than by directly promoting *SPL9* transcription. To determine whether the effect of *arp6* and *sef* on *MIR156A* and *MIR156C* expression is attributable to their role in the deposition of H2A.Z, we examined the abundance of pri-miR156a and pri-miR156c in the H2A.Z mutants *hta9-1*, *hta11-2* and *hta9-1 hta11-2*. Individually, *hta9-1* and *hta11-2* did not produce a significant decrease in the level of these transcripts; however, *hta9 hta11* mutants had ∼60% of the wild-type level of both pri-miR156a and pri-miR156c (Fig. 2F), which is approximately the same amount as in *arp6* and *sef* (Fig. 2B). These results support the hypothesis that the effect of *arp6* and *sef* on the expression of *MIR156A* and *MIR156C* is attributable to the loss of H2A.Z at these loci.

To test this hypothesis, we measured the level of H2A.Z at *MIR156A* and *MIR156C* in Col and *arp6* using chromatin immunoprecipitation (ChIP). Chromatin was isolated from 1-week-old seedlings and was immunoprecipitated with an antibody to H2A.Z; sites from across the promoter and transcribed regions of these genes were then amplified by PCR. H2A.Z was enriched in the first 500 nt after the transcription start site of both genes, but was relatively low in the promoter and towards the 3′ end of these genes (Fig. 3A,B). *arp6* seedlings had significantly reduced levels of H2A.Z at *MIR156A* and *MIR156C*, supporting the hypothesis that its effect on their expression is attributable to the loss of H2A.Z. We then asked if H2A.Z contributes to the downregulation of *MIR156A* and *MIR156C* during development by measuring the abundance of H2A.Z at these genes at 1, 2 and 3 weeks after planting. There was no significant change in the level of H2A.Z at these genes over this time period (Fig. 3C,D). The abundance of *ARP6* and *SEF* transcripts also did not change significantly during the first five weeks of growth (Fig. S1). Thus, variation in the abundance of H2A.Z or SWR1-C does not account for the major decrease in the expression of *MIR156A* and *MIR156C* during vegetative phase change.

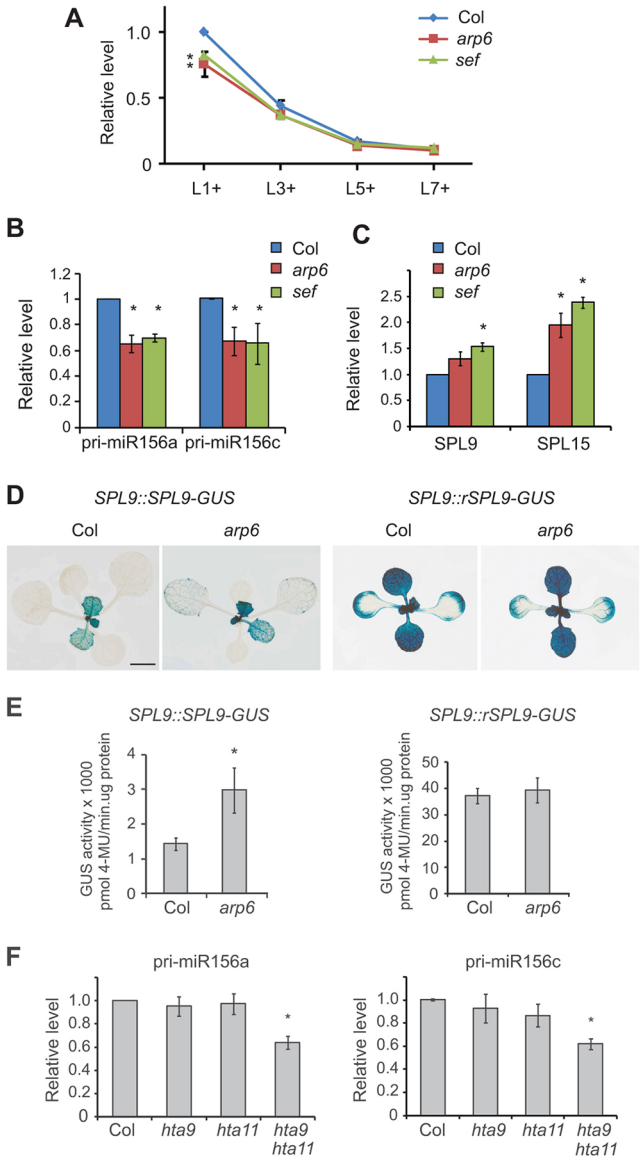

Fig. 2. SWR1-C activates *MIR156A* and *MIR156C* transcription in young seedlings. (A) RT-qPCR analysis of the abundance of miR156 in the shoot apices of Col, *arp6* and *sef* grown under short-day (SD) conditions. **P*<0.05, two-tailed Welch's *t*-test with Bonferroni adjustment. (B) RT-qPCR analysis of pri-miR156a and pri-miR156c in the shoot apex of 1-week-old seedlings grown under SD conditions. **P*<0.05, one-tailed Mann–Whitney *U*-test with Bonferroni adjustment. (C) RT-qPCR analysis of *SPL9* and *SPL15* mRNA in the shoot apex of 1-week-old seedlings grown under SD conditions. **P*<0.05, one-tailed Mann–Whitney *U*-test with Bonferroni adjustment. (D) GUS expression in 2-week-old Col and *arp6* plants containing genomic constructs encoding miR156-sensitive (*pSPL9::SPL9 -GUS*) or miR156-insensitive (*pSPL9::rSPL9-GUS*) SPL9-GUS fusion proteins. Scale bar: 2 mm. **P*<0.05, two-tailed Student's *t*-test. (E) MUG assays of GUS activity in the plants shown in D. (F) RT-qPCR analysis of pri-miR156a and pri-miR156c in Col, *hta9*, *hta11* and *hta9 hta11* mutants. **P*<0.05, Tukey's HSD test. Data are presented as the mean of three to five biological replicates±s.e.m.

ARP6 promotes the addition of H3K4me3 to *MIR156A* and *MIR156C*

To determine how SWR1-C promotes the expression of *MIR156A* and *MIR156C* we examined the effect of *arp6* on the active chromatin mark H3K4me3 and the repressive chromatin mark H3K27me3, and on nucleosome occupancy. We first examined the

Development (2018) 145, dev152868. doi:10.1242/dev.152868

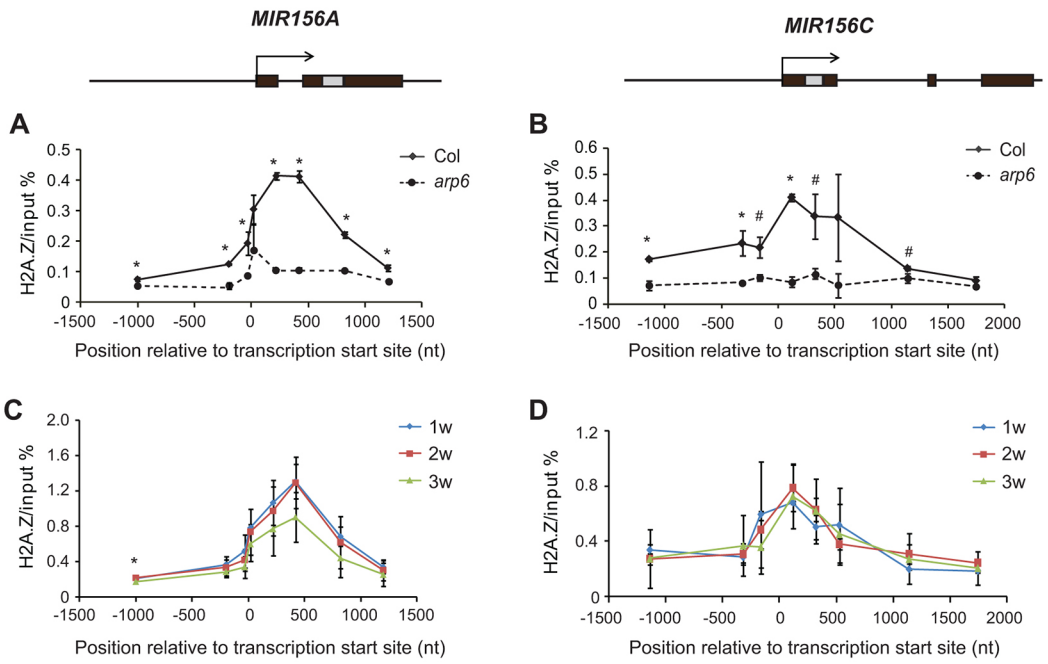

Fig. 3. ARP6 deposits H2A.Z at *MIR156A* and *MIR156C*. (A,B) ChIP analysis of H2A.Z levels at *MIR156A* (A) and *MIR156C* (B) in shoot apices of 1-week-old Col and *arp6-1* grown under short-day (SD) conditions. **P*<0.05, #*P*<0.1, one-tailed *t*-test or Welch's *t*-test. (C,D) ChIP analysis of H2A.Z levels at *MIR156A* (C) and *MIR156C* (D) in shoot apices of 1-, 2- and 3-week-old Col grown under SD conditions, **P*<0.05, one-way ANOVA. Graphs are aligned to the genomic structures of *MIR156A* and *MIR156C*, which are shown at the top of the figure. Black bars indicate exons; the gray boxes indicate the miR156 hairpin. Data are presented as the mean of two biological replicates±s.e.m.

temporal pattern of H3K4me3 and H3K27me3 deposition in wild-type plants. Chromatin from 1-, 2-, 3- and 5-week-old plants was immunoprecipitated with antibodies to H3K4me3 or H3K27me3, and DNA from these samples was then amplified using primers for sites in the promoter and coding regions of *MIR156A* and *MIR156C*. The results were normalized to the results obtained using antibodies to H3. Consistent with previous results (Xu et al., 2016a), we observed low levels of H3K27me3 in the promoter and transcribed region of *MIR156A*/*MIR156C* at 1 week, and this mark increased gradually at subsequent time points; it increased more rapidly and to a higher level at *MIR156A* than at *MIR156C* (Fig. 4A,B). H3K4me3 was confined to the transcribed regions of *MIR156A* and *MIR156C*, and was most abundant in a 750 nt region downstream of the transcription start site (Fig. 4C,D). At *MIR156A*, H3K4me3 decreased gradually from 1 to 5 weeks, whereas at *MIR156C*, it started to decline 2 weeks after planting and continued to decline thereafter. In summary, at *MIR156A* the abundance of H3K27me3 and H3K4me3 changed in a complementary fashion, whereas at *MIR156C* an increase in H3K27me3 preceded a decrease in H3K4me3.

arp6 reduced the level of H3K4me3 at both *MIR156A* and *MIR156C* in 1-week-old seedlings (Fig. 5A,B), and produced elevated levels of H3K27me3 at *MIR156A* (Fig. 5C). However, it had no effect on the level of H3K27me3 at *MIR156C* (Fig. 5D). To determine the effect of *arp6* on nucleosome occupancy, we examined the sensitivity of *MIR156A* and *MIR156C* chromatin to micrococcal nuclease (MNase), which preferentially cleaves naked DNA. Chromatin from 1-week-old *arp6* and wild-type seedlings was treated with MNase, and sites in a 600 bp region surrounding the transcription start sites of *MIR156A* and *MIR156C* were then assayed by qPCR. *arp6* increased MNase sensitivity at the site of the +1 nucleosome in *MIR156A* (~50-100 nt), but had no effect on MNase sensitivity upstream or downstream of this site (Fig. 5E). It had no effect on MNase sensitivity at *MIR156C* (Fig. 5F). These results suggest that H2A.Z promotes the expression of *MIR156A* and *MIR156C* primarily by promoting the deposition of H3K4me3, rather than by blocking the deposition of H3K27me3 or destabilizing the +1 nucleosome.

H3K4me3 and H3K27me3 are regulated independently by ARP6

The observation that *arp6* reduces H3K4me3 at both *MIR156A* and *MIR156C* (Fig. 5A,B), but only increases H3K27me3 at *MIR156A* (Fig. 5C,D) prompted us to study how *arp6* affects other genes that have both of these modifications. We analyzed five genes – *FLC*, *FT*, *APETALA1* (*AP1*), *NOZZLE* (*NZZ*) and *MALE STERILITY1* (*MS1*) – using *ACT7* and *STM* as positive controls for H3K4me3 and H3K27me3, respectively (Berr et al., 2010, 2015; Jiang et al., 2008; Saleh et al., 2007, 2008; Shafiq et al., 2014; Tamada et al., 2009; Yang et al., 2014; Yun et al., 2012). ChIP of extracts from 1-week-old seedlings, followed by qPCR of a site close to the transcription start site (TSS) and a site downstream of the TSS (Fig. 6A) showed that *arp6* significantly reduced H3K4me3 at most of these genes (Fig. 6B), but barely had any effect on H3K27me3 (Fig. 6C). Consistent with previous studies (Saleh et al., 2008; Tamada et al., 2009), the decrease in H3K4me3 at *FLC* was associated with significant decrease in its expression (Fig. 6D). *arp6* had no significant effect on the expression of *AP1*, *NZZ* and *MS1* (Fig. 6D), but this is not surprising because these genes are involved in floral morphogenesis and are expressed at extremely low levels in the 1-week-old seedlings used for this analysis; in the absence of the transcription factors necessary for the expression of these genes, a decrease in H3K4me3 is unlikely to have an effect on their expression. The expression of *FT* was upregulated in *arp6*, probably because of the downregulation of *FLC*, which is a strong repressor of *FT* (Helliwell et al., 2006; Michaels et al., 2005). To determine

Development (2018) 145, dev152868. doi:10.1242/dev.152868

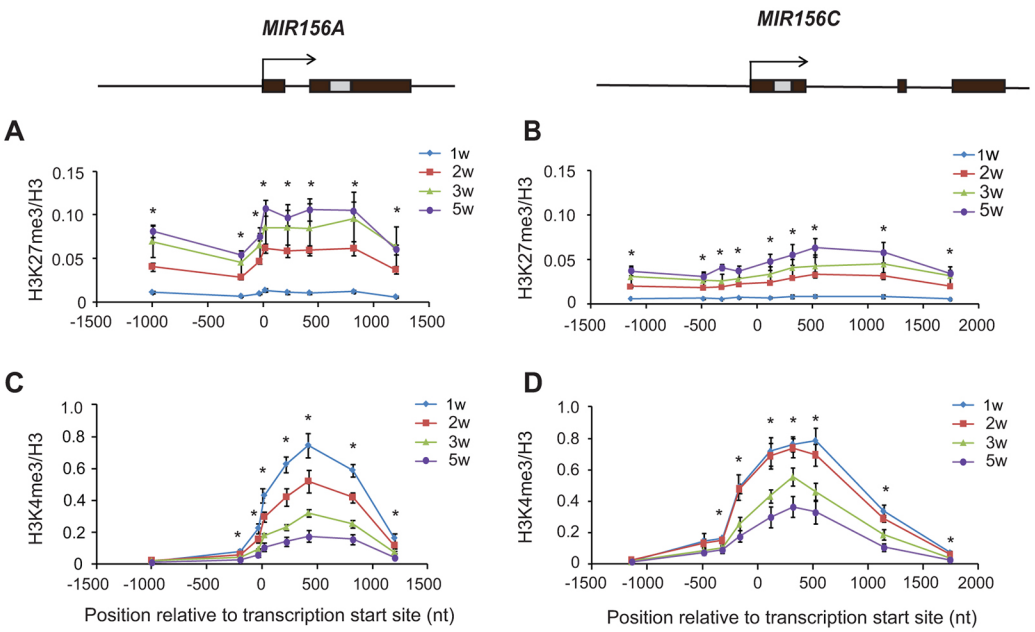

Fig. 4. H3K27me3 and H3K4me3 change in opposite directions at *MIR156A* and *MIR156C* during shoot development. (A,B) ChIP analysis of the abundance of H3K27me3 at *MIR156A* (A) and *MIR156C* (B) in the shoot apices of 1-, 2-, 3- and 5-week-old Col plants grown under short-day (SD) conditions. (C,D) ChIP analysis of the abundance of H3K4me3 at *MIR156A* (C) and *MIR156C* (D) in the shoot apices of 1-, 2-, 3- and 5-week-old Col plants grown under SD conditions. Data are the ratio of H3K27me3 or H3K4me3 relative to H3, and are the mean of three biological replicates±s.e.m. Graphs are aligned with the genomic structure of *MIR156A* and *MIR156C*, which is shown at the top of the figure. **P*<0.05, one-way ANOVA. Black bars indicate the exons; gray boxes indicate the miR156 hairpin.

whether *arp6* has a global effect on H3K4me3 and H3K27me3, we measured the abundance of these marks in Col and mutant seedlings using western blots. We observed no significant difference between these genotypes (Fig. 6E), suggesting that ARP6 only affects the deposition of H3K4me3 and H3K27me3 at some of the genes that possess these marks.

MIR156A and *MIR156C* are targets of the H3K4 methyltransferase ATXR7

To determine whether the effect of SWR1-C on vegetative phase change can be explained by its effect on H3K4me3, we examined the phenotypes and genetic interactions between *arp6*, *sef* and mutations in H3K4 methyl transferases. Phylogenetic analysis demonstrates that H3K4 methyl transferases in *Arabidopsis* can be classified into two groups, Trithorax genes and SET1 genes (Avramova, 2009). *ARABIDOPSIS TRITHORAX1* (*ATX1*) and *ATX2* are members of the Trithorax family, and work together to promote the expression of floral homeotic genes (Alvarez-Venegas et al., 2003; Carles and Fletcher, 2009) and the expression of *FLC* (Pien et al., 2008; Tamada et al., 2009). *ATXR7* is the only member of the SET1 subfamily in *Arabidopsis*, and functions along with *ATX1* and *ATX2* to promote the expression of *FLC* (Tamada et al., 2009).

The vegetative phenotypes of the single mutants *atx1-1*, *atx2-1*, *atxr7-1*, *arp6* and *sef*-2, and the phenotypes of plants bearing combinations of these mutations, were compared under both LD and SD conditions. *atx1-1* (hereafter, *atx1*), *atx2-1* (hereafter, *atx2*) and the *atx1 atx2* double mutant had no significant effect on leaf shape or on the timing of abaxial trichome production under both LD and SD (Fig. S2). In addition, neither mutation significantly enhanced the early abaxial trichome phenotype of *arp6* or *sef* in double mutants (Fig. S2C-F). The *atx1 atx2 arp6* and the *atx1 atx2 sef* triple mutants were embryonic lethal, making it impossible to determine the effect of these genotypes on vegetative phase change.

atxr7-1 (hereafter, *atxr7*), did not have an obvious effect on leaf shape (Fig. 7A), but produced leaves with abaxial trichomes approximately one leaf earlier than wild type; in this respect, it had approximately the same phenotype as *arp6* and *sef* (Fig. 7B). The double mutants *arp6 atxr7* and *sef atxr7* had more elongated and serrated leaves than the single mutants (Fig. 7A), and also produced abaxial trichomes significantly earlier than the single mutants (Fig. 7B). By comparison, the timing of abaxial trichome production in the *atx1 atx2 atxr7* triple mutant was not significantly different from *atxr7*, although this triple mutant had significantly more elongated leaves than *atxr7* (Fig. S2A,B). RT-qPCR analysis of 1-week old seedlings revealed that *arp6*, *sef* and *atxr7* had reduced levels of pri-miR156a and pri-miR156c, whereas *arp6 atxr7* had significantly lower levels of pri-miR156a than the single mutants (Fig. 7D,E). However, the level of pri-miR156c in *arp6 atxr7* was not significantly different from *arp6*.

To determine how ATXR7 regulates the expression of *MIR156A* and *MIR156C*, we used ChIP to measure the level of H3K4me3 and H3K27me3 in *atxr7* and wild-type seedlings. *atxr7* produced lower levels of H3K4me3 within the transcribed region of both *MIR156A* and *MIR156C* (Fig. 7F,G), but had a more reproducible effect at *MIR156A* than at *MIR156C*; it had no effect on the abundance of H3K27me3 at these loci (Fig. 7H,I). This result further demonstrates that the deposition of H3K4me3 and H3K27me3 is regulated independently at these genes. We then examined whether ATXR7 binds directly to *MIR156A* and *MIR156C* by taking advantage of a transgenic line expressing an ATXR7-GFP fusion protein under the regulation of the *ATXR7* promoter (Tamada et al., 2009). ChIP revealed that ATXR7-GFP binds adjacent to the transcription start site of *MIR156A* (Fig. 8A), at a position and with an affinity that are nearly identical to that reported at *FLC* using the same transgenic line (Tamada et al., 2009). The results of our RT-qPCR analysis were considerably more variable for *MIR156C* than

Development (2018) 145, dev152868. doi:10.1242/dev.152868

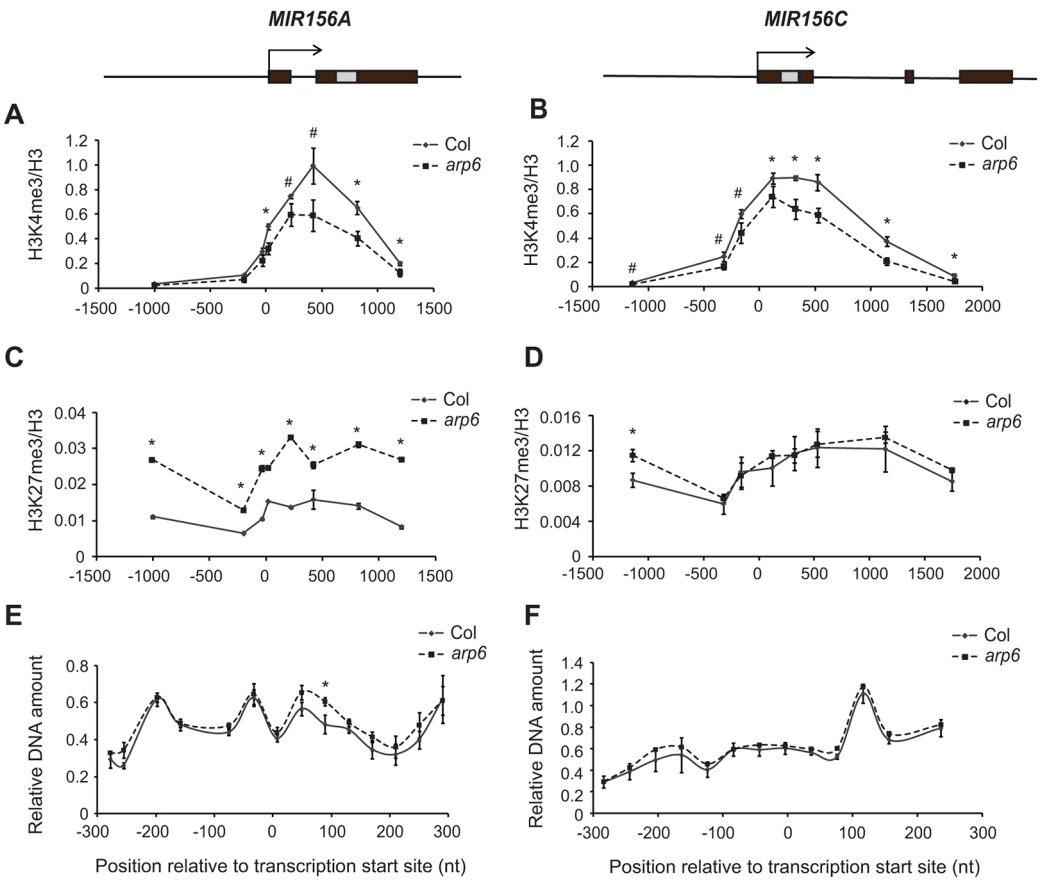

Fig. 5. *arp6* has the same effect on H3K4me3, but different effects on H3K27me3 and nucleosome occupancy, at *MIR156A* and *MIR156C*. (A,B) ChIP analysis of H3K4me3 levels at *MIR156A* (A) and *MIR156C* (B) in the shoot apices of 1-week-old Col and *arp6* seedlings. (C,D) ChIP analysis of H3K27me3 at *MIR156A* (C) and *MIR156C* (D) in the shoot apices Col and *arp6* seedlings. The data in A-D are presented as the ratio of H3K4me3 or H3K27me3 to H3 and are aligned with the diagrams of the genomic structure of *MIR156A* and *MIR156C*, shown at the top of the figure; data are the mean of three biological replicates ±s.e.m. **P*<0.05, #*P*<0.1, one-tailed *t*-test or Welch's *t*-test. (E,F) MNase assay of *MIR156A* (E) and *MIR156C* (F) chromatin. Data represent the amount of *MIR156A* (or *MIR156C*) DNA, relative to the amount of DNA from the −73 fragment of At4G07700, as determined by qPCR. Data are mean±s.e.m. from two biological replicates. **P*<0.05, one-tailed *t*-test. Graphs are not aligned with the diagrams of the genomic structure of *MIR156A* and *MIR156C*.

for *MIR156A*, and we did not observe significant binding of ATXR7 to *MIR156C* (Fig. 8B). This observation, and our observation that *atxr7* has a smaller effect on the expression of *MIR156C* and the level of H3K4me3 at *MIR156C* than at *MIR156A* (Fig. 8D-G), indicates that ATXR7 is more important for the regulation of *MIR156A* than *MIR156C*, and suggests that ATXR7 may associate only transiently with *MIR156C*.

DISCUSSION

miR156 promotes juvenile development by repressing the expression of a group of SBP/SPL transcription factors that promote the expression of the adult phase (Wu et al., 2009a; Xu et al., 2016a). The transition from the juvenile to the adult phase of vegetative development occurs when miR156 levels decrease sufficiently to allow these transcription factors to be expressed. Understanding the mechanism of this decrease is therefore essential for understanding the mechanism of vegetative phase change. Previously, we have shown that *MIR156A* and *MIR156C* are the major sources of miR156 in *Arabidopsis* (Yang et al., 2013), and that these genes are transcriptionally downregulated during vegetative phase by a decrease in the active histone modification H3K27ac and an increase in the level of H3K27me3 (Xu et al., 2016a). Here, we show that H3K4me3 also promotes the elevated expression of *MIR156A* and *MIR156C* early in shoot development, and that deposition of this mark is promoted by the presence of H2A.Z at these genes.

The molecular basis for the effect of H2A.Z on gene expression has been difficult to decipher because this histone can have positive or negative effects on transcription. In *Arabidopsis*, H2A.Z stabilizes nucleosomes and represses transcription at genes involved in defense, drought and temperature responses (Coleman-Derr and Zilberman, 2012; March-Díaz et al., 2008; Sura et al., 2017), but destabilizes nucleosomes and promotes gene expression at the *FLC* locus (Choi et al., 2005, 2007; Deal et al., 2005, 2007; Lázaro et al., 2008; March-Díaz et al., 2007, 2008; Martin-Trillo et al., 2006), and at the thalional and merneral metabolic gene clusters (Nützmann and Osbourn, 2015). Although mutations that affect the deposition of H2A.Z can affect the expression of genes involved in developmental transitions and the response to various environmental conditions, these developmental or environmental factors do not necessarily produce changes in the abundance of this histone (Hu et al., 2011). These observations have led to the conclusion that H2A.Z sensitizes genes to the activity of other factors that regulate transcription, but does not by itself promote or repress gene expression (Deal et al., 2007; Kumar and Wigge, 2010). Our results support this hypothesis. Specifically, we found that H2A.Z levels do not change significantly at *MIR156A* and *MIR156C* during vegetative phase change, and that the temporal expression pattern of miR156 is not significantly

Development (2018) 145, dev152868. doi:10.1242/dev.152868

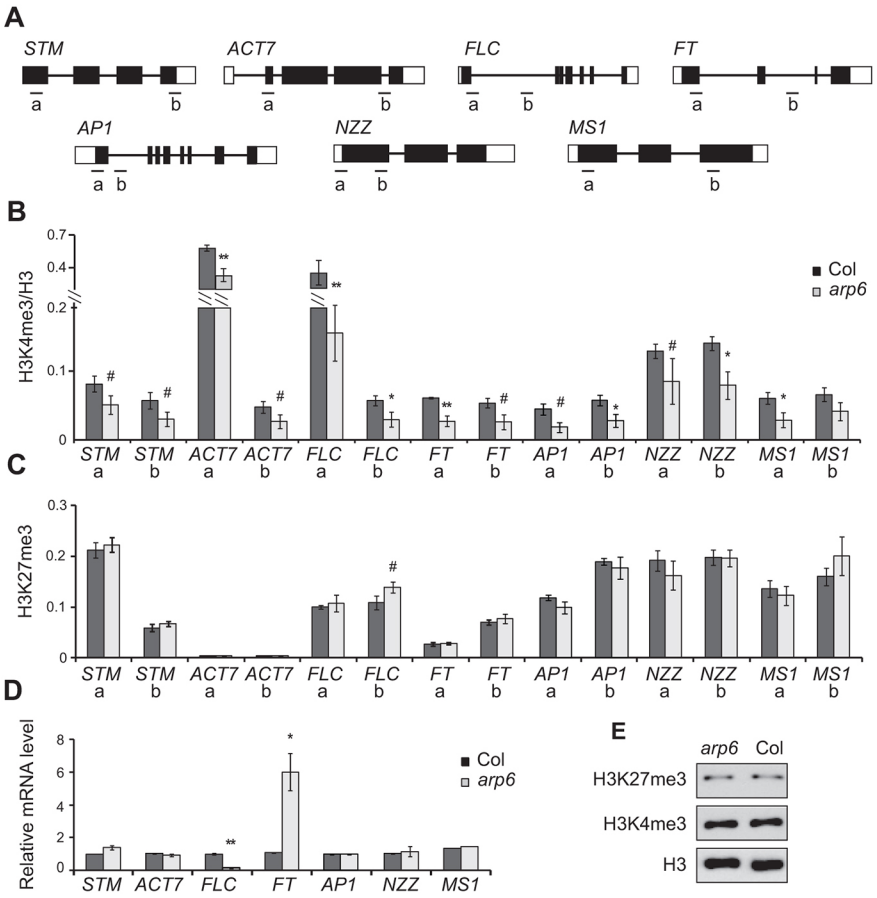

Fig. 6. ARP6 promotes the deposition of H3K4me3 at some bivalent genes, but does not have a significant effect on the global level of H3K4me3. (A) Schematic diagrams of the genomic structure of *STM*, *ACT7*, *FLC*, *FT*, *AP1*, *NZZ* and *MS1*. Black boxes indicate exons; white boxes indicate UTRs. (B,C) ChIP analysis of the abundance of H3K4me3 (B) and H3K27me3 (C) in the shoot apex of 1-week-old Col and *arp6* seedlings. $^{**}P<0.01$, $^{*}P<0.05$, $^{\#}P<0.1$, one-tailed *t*-test. (D) RT-qPCR analysis of mRNA abundance in the shoot apex of 1-week-old Col and *arp6*. The data for *arp6* are relative to the transcript abundance in Col, which was set to set to 1. $^{**}P<0.01$, $^{*}P<0.05$, two-tailed *t*-test. Data are the mean of three biological replicates ±s.e.m. (E) Western blot of protein extracts from 1-week-old Col and *arp6-1* seedlings probed with antibodies to H3K4me3, H3K27me3 and H3.

affected by the loss of H2A.Z in *arp6*. The simplest interpretation of this observation is that H2A.Z sensitizes *MIR156A* and *MIR156C* to factors that promote transcription without inhibiting their accessibility to temporally regulated factors that repress their transcription. Although H2A.Z does not play a major role in the repression of *MIR156A* and *MIR156C* transcription during vegetative phase change, it may be important for the upregulation of miR156 expression during embryogenesis, when the abundance of this miRNA increases to very high levels (Nodine and Bartel, 2010). The reactivation of *FLC* expression during embryogenesis requires the activity of PIE1, a component of SWR1-C (Choi et al., 2009), and perhaps the reactivation of *MIR156A* and/or *MIR156C* expression during embryogenesis also depends on this complex.

A previous study of the effect of *arp6* on miRNA gene expression concluded that ARP6 promotes the expression of *MIR156A* by reducing nucleosome occupancy at this locus (Choi et al., 2016). We confirmed the observation that *arp6* increases nucleosome occupancy at *MIR156A*, but found that it had no effect on nucleosome occupancy at *MIR156C*. Similarly, *arp6* increased the level of H3K27me3 at *MIR156A*, but had no effect on this mark at *MIR156C*. The only effect that was common to both genes was a reduction in the abundance of H3K4me3. We also found that *arp6* reduced H3K4me3 at *FLC*, *FT*, *AP1*, *NZZ* and *MS1*. Importantly, the loss of H3K4me3 at *MIR156C*, *FLC*, *FT*, *AP1*, *NZZ* and *MS1* was not accompanied by a change in the level of H3K27me3 at these genes. Furthermore, although *arp6* reduced the transcription of *MIR156A*, *MIR156C* and *FLC*, it did not affect the transcription of *AP1*, *NZZ* and *MS1* in the 1-week-old seedlings used for this analysis. *AP1*, *NZZ* and *MS1* are involved in floral differentiation or gametophyte development (Berr et al., 2010; Mandel and Yanofsky, 1995; Wagner et al., 1999) and are expressed at very low levels in 1-week-old seedlings. It is therefore not surprising that the loss of H3K4me3 is not associated with an increase in H3K27me3 or further decrease in their expression at this stage. It remains to be determined whether *arp6* affects their expression in the inflorescence and flowers, where they are normally expressed. Whatever the case, these observations suggest that ARP6 and, by extension, H2A.Z, directly promotes the deposition of H3K4me3, and that this is the primary mechanism by which it regulates the expression of *MIR156A* and *MIR156C*.

In mammalian embryonic stem cells, H2A.Z facilitates the binding of the H3K4 methyltransferase MLL, a homolog of the *Trithorax* gene in *Drosophila* (Creyghton et al., 2008; Hu et al., 2013). We found that mutations in the H3K4 methyltransferase gene *ATXR7* decrease the level of H3K4me3 at *MIR156A* and *MIR156C*, and have a phenotype similar to *arp6* and *sef*, making it an excellent candidate for an H2A.Z-interacting protein. Whether or not H2A.Z acts by affecting the accessibility of *MIR156A* and *MIR156C* to ATXR7, it is clear that ATXR7 is not the only H3K4 methyl transferase that operates at these loci because *arp6 atxr7* and *sef atxr7* double mutants have a more severe phase change phenotype than the single mutations. *atx1* and *atx2* did not have an obvious effect on phase change, but the *atxr7 atx1 atx2* triple mutant had a stronger leaf shape phenotype than *atxr7*, suggesting that these TrX proteins may also operate at *MIR156A* and *MIR156C*. Although H2A.Z may facilitate the activity of these or other H3K4 methyltransferases, the evidence that H3K4me3 decreases at

Development (2018) 145, dev152868. doi:10.1242/dev.152868

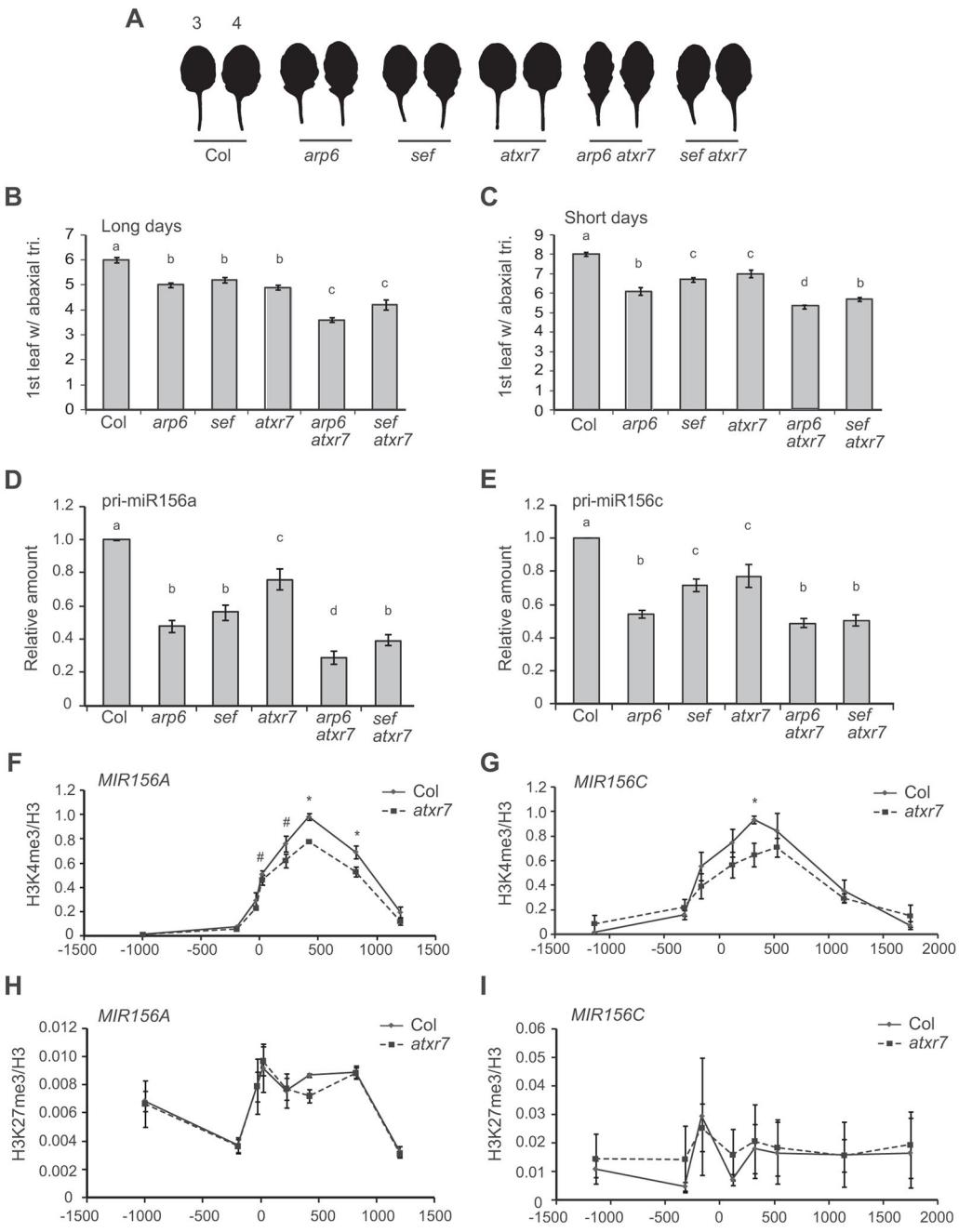

Fig. 7. ATXR7 promotes the expression of *MIR156A* and *MIR156C*. (A) Morphology of leaf 3 and leaf 4 in Col, *arp6*, *sef* and *atxr7*. (B,C) The first leaf with abaxial trichomes in Col and mutant rosettes under long-day (LD) (B) and short-day (SD) (C) conditions. *n*=20-24. (D,E) RT-qPCR analysis of pri-miR156a (D) and pri-miR156c. (E) levels in the shoot apices of 1-week-old Col and mutant seedlings. Letters above the bars indicate significant difference at $P<0.05$, Tukey's HSD test. Samples with different letters are significantly different. (F,G) ChIP analysis of the abundance of H3K4me3 at *MIR156A* (F) and *MIR156C* (G) in the shoot apices of 1-week-old Col and *atxr7* seedlings. (H,I) ChIP analysis of the abundance of H3K27me3 at *MIR156A* (H) and *MIR156C* (I) in the shoot apices of 1-week-old Col and *atxr7* seedlings. $^{*}P<0.05$, $^{\#}P<0.1$, one-tailed *t*-test. The data in figures D-I are the mean of three biological replicates±s.e.m.

MIR156A and *MIR156C* in the absence of a change in H2A.Z or a change in the expression of *ARP6* or *SEF* indicates that these factors are not responsible for developmental variation in the deposition of H3K4me3 at *MIR156A* and *MIR156C*.

The transcription of genes that possess the active histone modification H3K4me3 and the repressive modification H3K27me3 is thought to be regulated by the balance between these marks (Pien et al., 2008), but how the relative abundance of these modifications is regulated is still unknown. At *FLC*, for example, mutations in the H3K4 methyltransferases *ATX1*, *ATXR3* and *ATX7* decrease H3K4me3 and simultaneously increase the level of H3K27me3 (Pien et al., 2008; Tamada et al., 2009; Yun et al., 2012), suggesting that these marks are mutually exclusive. However, *in vitro* studies indicate that, whereas H3K4me3 can inhibit the binding of PRC2 to nucleosomes, this effect depends on the subunit composition of PRC2. Complexes containing EMF2 are incapable of binding nucleosomes containing H3K4me3, but complexes containing VRN2 – a paralog of EMF2 – are capable of binding such nucleosomes (Schmitges et al., 2011). If *MIR156A* and *MIR156C* are bound by different isoforms of PRC2, this may explain why *arp6* decreased H3K4me3 at both *MIR156A* and *MIR156C*, but only increased H3K27me3 at *MIR156A*. The evidence that *MIR156C* expression is more significantly affected by mutations in the PRC2 component *SWN* than is *MIR156A* expression (Xu et al., 2016a) is consistent with the hypothesis that these loci are targeted by different forms of PRC2.

miR156 regulates many aspects of plant development, including the timing of vegetative phase change, flowering time, fruit development, the rate of leaf initiation, lateral root development, anthocyanin production, stress responses and shoot regeneration in

Development (2018) 145, dev152868. doi:10.1242/dev.152868

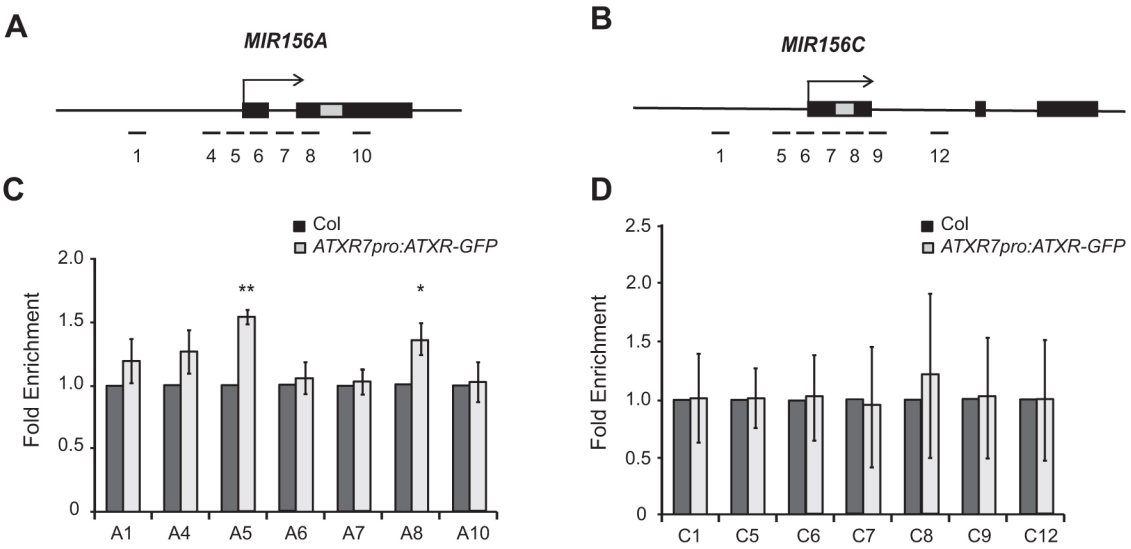

Fig. 8. ATXR7 binds to *MIR156A*. (A,B) Schematic diagram of the genomic structure of *MIR156A* and *MIR156C*, and the location of the PCR primers used in ChIP analysis. (C,D) ChIP of ATXR7-GFP at *MIR156A* and *MIR156C*. ATXR7-GFP was enriched at *MIR156A*, but we observed no significant enrichment at *MIR156C*. One-week-old *FRI* Col and *FRI ATXR7pro:ATXR7-GFP* #18 seedlings were cross-linked and chromatin was immunoprecipitated with an anti-GFP antibody. The abundance of different DNA fragments in the immunoprecipitated fraction was calculated as the percentage of input and normalized to TA3. $^{**}P<0.01$, $^{*}P<0.05$, two-tailed *t*-test. The data are the mean of three biological replicates±s.e.m.

tissue culture (Ferreira e Silva et al., 2014; Gou et al., 2011; Khan et al., 2014; Lei et al., 2016; Wang et al., 2009, 2008; Wu et al., 2009a; Wu and Poethig, 2006; Xing et al., 2010; Yu et al., 2015; Zhang et al., 2015). It is unknown whether all of these responses are regulated by *MIR156A* and *MIR156C*, or whether other members of this gene family are more important under certain conditions. In the context of the present study, this is an important issue because H2A.Z may have different functions at different *MIR156* genes, perhaps mediated by the unique histone methylation signatures at these loci. Determining the role of this histone in the many processes regulated by miR156 will be an important subject for future research.

MATERIALS AND METHODS

Plant materials and growth conditions

All of the stocks used in this study were in a Col background. *arp6*-1 (SAIL_599_G03), *arp6*-2 (SAIL_236_C07), *sef*-2 (SAIL_1142_C03), *hta9-1* (SALK_054814C), *hta11-2* (SALK_031471), *atx1-2* (SALK_149002), *atx2-1* (SALK_074806) and *atxr7-1* (SALK_149692C) were obtained from ABRC. Primers for genotyping these mutants are listed in Table S1. *mir156a-2* and *mir156c-1* have been described previously (Yang et al., 2013). The *ATXR7pro::ATXR7-GFP* line was a gift from Dr Richard M. Amasino (University of Wisconsin, Madison, USA). Seeds were stratified at 4°C for 2 to 4 days and then transferred to 22°C at day 1. For phenotypic analysis, plants were grown under long days (16 h light:8 h dark) or short days (10 h light:14 h dark) conditions at 22°C, under a combination of cool white and Gro-Lite WS (Interelectric) fluorescent lights. All qPCR and ChIP analyses were performed with plants grown under short day conditions.

RT-qPCR

Shoot apices of plants at different developmental stages or from 1-week-old whole seedlings were used for qPCR, as indicated in the text. Total RNA was isolated using TRIzol (Invitrogen), followed by TURBO DNase (Ambion) treatment, according to the manufacturer's instructions. RNA (1.2 µg) was used in reverse transcription with SuperScriptIII Reverse Transcriptase (Invitrogen). RT-qPCR was performed on BIO-RAD CFX96 Real time System. Quantitative analysis of mature miR156 transcripts and mRNAs of protein-coding genes was performed as described previously (Xu et al., 2016a) using the primers listed in Table S1.

Chromatin immunoprecipitation

One-, 2-, 3- and 5-week-old Col shoot apices (0.5 g) were harvested for the analysis of H3K4me3 and H3K27me3 abundance at *MIR156A* and *MIR156C*. One-week-old seedlings were used for a comparison of H3K4me3 and H3K27me3 deposition at these genes in Col and *arp6*. Chromatin immunoprecipitation was performed as described previously (Xu et al., 2016a) and the results were analyzed using the PCR primers described in this paper. Antibodies to H3 and H3K27me3 were purchased from Abcam (ab1791) and Millipore (07-449), respectively. The antibody against H3K4me3 was obtained from EMD (04-745). The H2A.Z antibody was a gift from Roger Deal (Emory University, Atlanta, GA, USA). The abundance of H3K27me3, H3K4me3 and H2A.Z was calculated as the ratio of H3K27me3/H3, H3K4me3/H3 or H2A.Z/H3. The GFP antibody was purchased from Clontech (632592). The fold-enrichment was calculated as the percentage of input and normalized to TA3, and the fold in Col was set to 1. The data are presented as the average of three biological replicates.

MNase assay

MNase assays were performed using 0.8 g of tissue from 1-week-old seedlings, as previously described (Xu et al., 2016a). Briefly, nuclei were isolated and treated with 0.1 U/µl micrococcal nuclease (Clontech, 2910) for 3-5 min. Mononucleosome DNA was then gel-purified using a Fisher GenJET gel extraction Kit. DNA amplification and the calculation of nucleosome occupancy were performed as described previously (Xu et al., 2016a).

Western blotting

Nuclei from 1-week-old Col and *arp6* seedlings were isolated according to Han and colleagues (2012). Nuclei proteins were released and separated by electrophoresis on a 15% SDS-PAGE gel. Immunoblots were performed using the anti-H3, anti-H3K4me3 and anti-H3K4me3 antibodies that were used for ChIP assays.

Statistical analyses

All statistical tests were conducted in R (R Core Team, 2015). The appropriateness of parametric tests were all confirmed by analyzing the distribution of the residuals and homogeneity of the variance from fitted linear models. In necessary cases, response variables were log transformed to meet parametric assumptions. Welch's *t*-test was used in cases where the assumption of equal variance was not met. Bonferroni adjustments were

made on *P* values derived from two or more comparisons. The multcomp package (Hothorn et al., 2008) was used for Dunnett's test. The BSDA package (Arnholt and Evans, 2017) was used for nonparametric Sign-Tests.

Acknowledgements
We are grateful to Roger Deal for antibodies against H2A.Z and to members of the Poethig laboratory for helpful discussions.

Competing interests
The authors declare no competing or financial interests.

Author contributions
Conceptualization: M.X.; Formal analysis: M.X., A.R.L., R.S.P.; Investigation: M.X., T.H.; Writing - original draft: M.X.; Writing - review & editing: M.X., R.S.P.; Supervision: R.S.P.; Project administration: R.S.P.; Funding acquisition: R.S.P.

Funding
This work was supported by a grant from the National Institutes of Health (GM51893). Deposited in PMC for release after 12 months.

Supplementary information
Supplementary information available online at
http://dev.biologists.org/lookup/doi/10.1242/dev.152868.supplemental

References

Abbott, D. W., Ivanova, V. S., Wang, X., Bonner, W. M. and Ausió, J. (2001). Characterization of the stability and folding of H2A.Z chromatin particles: implications for transcriptional activation. *J. Biol. Chem.* **276**, 41945-41949.

Alvarez-Venegas, R., Pien, S., Sadder, M., Witmer, X., Grossniklaus, U. and Avramova, Z. (2003). *ATX-1*, an *Arabidopsis* homolog of trithorax, activates flower homeotic genes. *Curr. Biol.* **13**, 627-637.

Arnholt, A. T. and Evans, B. (2017). BSDA: Basic Statistics and Data Analysis. R package version 1.2.0. https://CRAN.R-project.org/package=BSDA.

Avramova, Z. (2009). Evolution and pleiotropy of TRITHORAX function in *Arabidopsis*. *Int. J. Dev. Biol.* **53**, 371-381.

Berr, A., McCallum, E. J., Menard, R., Meyer, D., Fuchs, J., Dong, A. and Shen, W.-H. (2010). *Arabidopsis* SET DOMAIN GROUP2 is required for H3K4 trimethylation and is crucial for both sporophyte and gametophyte development. *Plant Cell* **22**, 3232-3248.

Berr, A., Shafiq, S., Pinon, V., Dong, A. and Shen, W.-H. (2015). The trxG family histone methyltransferase SET DOMAIN GROUP 26 promotes flowering via a distinctive genetic pathway. *Plant J.* **81**, 316-328.

Bowerman, S. and Wereszczynski, J. (2016). Effects of macroH2A and H2A.Z on nucleosome dynamics as elucidated by molecular dynamics simulations. *Biophys. J.* **110**, 327-337.

Carles, C. C. and Fletcher, J. C. (2009). The SAND domain protein ULTRAPETALA1 acts as a trithorax group factor to regulate cell fate in plants. *Genes Dev.* **23**, 2723-2728.

Cheng, C., Gao, X., Feng, B., Sheen, J., Shan, L. and He, P. (2013). Plant immune response to pathogens differs with changing temperatures. *Nat. Commun.* **4**, 2530.

Choi, K., Kim, S., Kim, S. Y., Kim, M., Hyun, Y., Lee, H., Choe, S., Kim, S. G., Michaels, S. and Lee, I. (2005). *SUPPRESSOR OF FRIGIDA3* encodes a nuclear ACTIN-RELATED PROTEIN6 required for floral repression in *Arabidopsis*. *Plant Cell* **17**, 2647-2660.

Choi, K., Park, C., Lee, J., Oh, M., Noh, B. and Lee, I. (2007). *Arabidopsis* homologs of components of the SWR1 complex regulate flowering and plant development. *Development* **134**, 1931-1941.

Choi, J., Hyun, Y., Kang, M.-J., In Yun, H., Yun, J.-Y., Lister, C., Dean, C., Amasino, R. M., Noh, B., Noh, Y.-S. et al. (2009). Resetting and regulation of *FLOWERING LOCUS C* expression during *Arabidopsis* reproductive development. *Plant J.* **57**, 918-931.

Choi, K., Zhao, X., Kelly, K. A., Venn, O., Higgins, J. D., Yelina, N. E., Hardcastle, T. J., Ziolkowski, P. A., Copenhaver, G. P., Franklin, F. C. H. et al. (2013). *Arabidopsis* meiotic crossover hot spots overlap with H2A.Z nucleosomes at gene promoters. *Nat. Genet.* **45**, 1327-1336.

Choi, K., Kim, J., Müller, S. Y., Oh, M., Underwood, C., Henderson, I. and Lee, I. (2016). Regulation of microRNA-mediated developmental changes by the SWR1 chromatin remodeling complex. *Plant Physiol.* **171**, 1128-1143.

Coleman-Derr, D. and Zilberman, D. (2012). Deposition of histone variant H2A.Z within gene bodies regulates responsive genes. *PLoS Genet.* **8**, e1002988.

Creyghton, M. P., Markoulaki, S., Levine, S. S., Hanna, J., Lodato, M. A., Sha, K., Young, R. A., Jaenisch, R. and Boyer, L. A. (2008). H2AZ is enriched at polycomb complex target genes in ES cells and is necessary for lineage commitment. *Cell* **135**, 649-661.

Deal, R. B., Kandasamy, M. K., McKinney, E. C. and Meagher, R. B. (2005). The nuclear actin-related protein ARP6 is a pleiotropic developmental regulator required for the maintenance of *FLOWERING LOCUS C* expression and repression of flowering in *Arabidopsis*. *Plant Cell* **17**, 2633-2646.

Deal, R. B., Topp, C. N., McKinney, E. C. and Meagher, R. B. (2007). Repression of flowering in *Arabidopsis* requires activation of *FLOWERING LOCUS C* expression by the histone variant H2A.Z. *Plant Cell* **19**, 74-83.

Ferreira e Silva, G. F., Silva, E. M., da Silva Azevedo, M., Guivin, M. A. C., Ramiro, D. A., Figueiredo, C. R., Carrer, H., Peres, L. E. P. and Nogueira, F. T. S. (2014). microRNA156-targeted SPL/SBP box transcription factors regulate tomato ovary and fruit development. *Plant J.* **78**, 604-618.

Gou, J.-Y., Felippes, F. F., Liu, C.-J., Weigel, D. and Wang, J.-W. (2011). Negative regulation of anthocyanin biosynthesis in *Arabidopsis* by a miR156-targeted SPL transcription factor. *Plant Cell* **23**, 1512-1522.

Han, S.-K., Sang, Y., Rodrigues, A., BIOL425 F2010, Wu, M.-F., Rodriguez, P. L. and Wagner, D. (2012). The SWI2/SNF2 chromatin remodeling ATPase BRAHMA represses abscisic acid responses in the absence of the stress stimulus in *Arabidopsis*. *Plant Cell* **24**, 4892-4906.

Helliwell, C. A., Wood, C. C., Robertson, M., James Peacock, W. and Dennis, E. S. (2006). The *Arabidopsis* FLC protein interacts directly in vivo with *SOC1* and *FT* chromatin and is part of a high-molecular-weight protein complex. *Plant J.* **46**, 183-192.

Hoch, D. A., Stratton, J. J. and Gloss, L. M. (2007). Protein-protein Förster resonance energy transfer analysis of nucleosome core particles containing H2A and H2A.Z. *J. Mol. Biol.* **371**, 971-988.

Hong, J., Feng, H., Wang, F., Ranjan, A., Chen, J., Jiang, J., Ghirlando, R., Xiao, T. S., Wu, C. and Bai, Y. (2014). The catalytic subunit of the SWR1 remodeler is a histone chaperone for the H2A.Z-H2B dimer. *Mol. Cell* **53**, 498-505.

Hothorn, T., Bretz, F. and Westfall, P. (2008). Simultaneous inference in general parametric models. *Biom. J.* **50**, 346-363.

Hu, Y., Shen, Y., Conde e Silva, N. and Zhou, D.-X. (2011). The role of histone methylation and H2A.Z occupancy during rapid activation of ethylene responsive genes. *PLoS ONE* **6**, e28224.

Hu, G., Cui, K., Northrup, D., Liu, C., Wang, C., Tang, Q., Ge, K., Levens, D., Crane-Robinson, C. and Zhao, K. (2013). H2A.Z facilitates access of active and repressive complexes to chromatin in embryonic stem cell self-renewal and differentiation. *Cell Stem Cell* **12**, 180-192.

Jiang, D., Wang, Y., Wang, Y. and He, Y. (2008). Repression of *FLOWERING LOCUS C* and *FLOWERING LOCUS T* by the *Arabidopsis* Polycomb repressive complex 2 components. *PLoS ONE* **3**, e3404.

Jin, C. and Felsenfeld, G. (2007). Nucleosome stability mediated by histone variants H3.3 and H2A.Z. *Genes Dev.* **21**, 1519-1529.

Khan, M. R. G., Ai, X.-Y. and Zhang, J.-Z. (2014). Genetic regulation of flowering time in annual and perennial plants. *Wiley Interdiscip. Rev. RNA* **5**, 347-359.

Kruger, W., Peterson, C. L., Sil, A., Coburn, C., Arents, G., Moudrianakis, E. N. and Herskowitz, I. (1995). Amino acid substitutions in the structured domains of histones H3 and H4 partially relieve the requirement of the yeast SWI/SNF complex for transcription. *Genes Dev.* **9**, 2770-2779.

Kumar, S. V. and Wigge, P. A. (2010). H2A.Z-containing nucleosomes mediate the thermosensory response in *Arabidopsis*. *Cell* **140**, 136-147.

Lázaro, A., Gómez-Zambrano, A., López-González, L., Piñeiro, M. and Jarillo, J. A. (2008). Mutations in the *Arabidopsis SWC6* gene, encoding a component of the SWR1 chromatin remodelling complex, accelerate flowering time and alter leaf and flower development. *J. Exp. Bot.* **59**, 653-666.

Lei, K. J., Lin, Y. M. and An, G. Y. (2016). miR156 modulates rhizosphere acidification in response to phosphate limitation in *Arabidopsis*. *J. Plant Res.* **129**, 275-284.

Lu, P. Y. T., Lévesque, N. and Kobor, M. S. (2009). NuA4 and SWR1-C: two chromatin-modifying complexes with overlapping functions and components. *Biochem. Cell Biol.* **87**, 799-815.

Mandel, M. A. and Yanofsky, M. F. (1995). A gene triggering flower formation in *Arabidopsis*. *Nature* **377**, 522-524.

March-Díaz, R., Garcia-Dominguez, M., Florencio, F. J. and Reyes, J. C. (2007). SEF, a new protein required for flowering repression in *Arabidopsis*, interacts with PIE1 and ARP6. *Plant Physiol.* **143**, 893-901.

March-Díaz, R., García-Domínguez, M., Lozano-Juste, J., León, J., Florencio, F. J. and Reyes, J. C. (2008). Histone H2A.Z and homologues of components of the SWR1 complex are required to control immunity in *Arabidopsis*. *Plant J.* **53**, 475-487.

Martin-Trillo, M., Lazaro, A., Poethig, R. S., Gomez-Mena, C., Pineiro, M. A., Martinez-Zapater, J. M. and Jarillo, J. A. (2006). *EARLY IN SHORT DAYS 1* (*ESD1*) encodes ACTIN-RELATED PROTEIN 6 (AtARP6), a putative component of chromatin remodelling complexes that positively regulates FLC accumulation in *Arabidopsis*. *Development* **133**, 1241-1252.

Michaels, S. D., Himelblau, E., Kim, S. Y., Schomburg, F. M. and Amasino, R. M. (2005). Integration of flowering signals in winter-annual *Arabidopsis*. *Plant Physiol.* **137**, 149-156.

Mizuguchi, G., Shen, X., Landry, J., Wu, W. H., Sen, S. and Wu, C. (2004). ATP-driven exchange of histone H2A.Z variant catalyzed by SWR1 chromatin remodeling complex. *Science* **303**, 343-348.

Morrison, A. J. and Shen, X. (2009). Chromatin remodelling beyond transcription: the INO80 and SWR1 complexes. *Nat. Rev. Mol. Cell Biol.* **10**, 373-384.
Nodine, M. D. and Bartel, D. P. (2010). MicroRNAs prevent precocious gene expression and enable pattern formation during plant embryogenesis. *Genes Dev.* **24**, 2678-2692.
Nützmann, H.-W. and Osbourn, A. (2015). Regulation of metabolic gene clusters in *Arabidopsis thaliana*. *New Phytol.* **205**, 503-510.
Picó, S., Ortiz-Marchena, M. I., Merini, W. and Calonje, M. (2015). Deciphering the role of POLYCOMB REPRESSIVE COMPLEX1 variants in regulating the acquisition of flowering competence in *Arabidopsis*. *Plant Physiol.* **168**, 1286-1297.
Pien, S., Fleury, D., Mylne, J. S., Crevillen, P., Inze, D., Avramova, Z., Dean, C. and Grossniklaus, U. (2008). ARABIDOPSIS TRITHORAX1 dynamically regulates *FLOWERING LOCUS C* activation via histone 3 lysine 4 trimethylation. *Plant Cell* **20**, 580-588.
Poethig, R. S. (2003). Phase change and the regulation of developmental timing in plants. *Science* **301**, 334-336.
Qin, Y., Zhao, L., Skaggs, M. I., Andreuzza, S., Tsukamoto, T., Panoli, A., Wallace, K. N., Smith, S., Siddiqi, I., Yang, Z. et al. (2014). ACTIN-RELATED PROTEIN6 Regulates female meiosis by modulating meiotic gene expression in *Arabidopsis*. *Plant Cell* **26**, 1612-1628.
R Core Team (2015). *R: A Language and Environment for Statistical Computing*. Vienna, Austria: R Foundation for Statistical Computing. https://www.R-project.org/.
Redon, C., Pilch, D., Rogakou, E., Sedelnikova, O., Newrock, K. and Bonner, W. (2002). Histone H2A variants H2A.X and H2A.Z. *Curr. Opin. Genet. Dev.* **12**, 162-169.
Rosa, M., Von Harder, M., Cigliano, R. A., Schlogelhofer, P. and Mittelsten Scheid, O. (2013). The *Arabidopsis* SWR1 chromatin-remodeling complex is important for DNA repair, somatic recombination, and meiosis. *Plant Cell* **25**, 1990-2001.
Saleh, A., Al-Abdallat, A., Ndamukong, I., Alvarez-Venegas, R. and Avramova, Z. (2007). The *Arabidopsis* homologs of trithorax (ATX1) and enhancer of zeste (CLF) establish 'bivalent chromatin marks' at the silent AGAMOUS locus. *Nucleic Acids Res.* **35**, 6290-6296.
Saleh, A., Alvarez-Venegas, R. and Avramova, Z. (2008). Dynamic and stable histone H3 methylation patterns at the *Arabidopsis* FLC and AP1 loci. *Gene* **423**, 43-47.
Schmitges, F. W., Prusty, A. B., Faty, M., Stützer, A., Lingaraju, G. M., Aiwazian, J., Sack, R., Hess, D., Li, L., Zhou, S. et al. (2011). Histone methylation by PRC2 is inhibited by active chromatin marks. *Mol. Cell* **42**, 330-341.
Shafiq, S., Berr, A. and Shen, W.-H. (2014). Combinatorial functions of diverse histone methylations in *Arabidopsis thaliana* flowering time regulation. *New Phytol.* **201**, 312-322.
Smith, A. P., Jain, A., Deal, R. B., Nagarajan, V. K., Poling, M. D., Raghothama, K. G. and Meagher, R. B. (2010). Histone H2A.Z regulates the expression of several classes of phosphate starvation response genes but not as a transcriptional activator. *Plant Physiol.* **152**, 217-225.
Sura, W., Kabza, M., Karlowski, W. M., Bieluszewski, T., Kus-Slowinska, M., Pawełoszek, Ł., Sadowski, J. and Ziolkowski, P. A. (2017). Dual role of the histone variant H2A.Z in transcriptional regulation of stress-response genes. *Plant Cell* **29**, 791-807.
Tamada, Y., Yun, J.-Y., Woo, S. C. and Amasino, R. M. (2009). *ARABIDOPSIS TRITHORAX-RELATED7* is required for methylation of lysine 4 of histone H3 and for transcriptional activation of *FLOWERING LOCUS C*. *Plant Cell* **21**, 3257-3269.
van Attikum, H., Fritsch, O. and Gasser, S. M. (2007). Distinct roles for SWR1 and INO80 chromatin remodeling complexes at chromosomal double-strand breaks. *EMBO J.* **26**, 4113-4125.
Wagner, D., Sablowski, R. W. and Meyerowitz, E. M. (1999). Transcriptional activation of *APETALA1* by LEAFY. *Science* **285**, 582-584.
Wang, J.-W., Schwab, R., Czech, B., Mica, E. and Weigel, D. (2008). Dual effects of miR156-targeted SPL genes and CYP78A5/KLUH on plastochron length and organ size in *Arabidopsis thaliana*. *Plant Cell* **20**, 1231-1243.
Wang, J.-W., Czech, B. and Weigel, D. (2009). miR156-regulated SPL transcription factors define an endogenous flowering pathway in *Arabidopsis thaliana*. *Cell* **138**, 738-749.
Willmann, M. R. and Poethig, R. S. (2011). The effect of the floral repressor *FLC* on the timing and progression of vegetative phase change in *Arabidopsis*. *Development* **138**, 677-685.
Wu, G. and Poethig, R. S. (2006). Temporal regulation of shoot development in *Arabidopsis thaliana* by miR156 and its target SPL3. *Development* **133**, 3539-3547.
Wu, W.-H., Alami, S., Luk, E., Wu, C.-H., Sen, S., Mizuguchi, G., Wei, D. and Wu, C. (2005). Swc2 is a widely conserved H2AZ-binding module essential for ATP-dependent histone exchange. *Nat. Struct. Mol. Biol.* **12**, 1064-1071.
Wu, G., Park, M. Y., Conway, S. R., Wang, J.-W., Weigel, D. and Poethig, R. S. (2009a). The sequential action of miR156 and miR172 regulates developmental timing in *Arabidopsis*. *Cell* **138**, 750-759.
Wu, W.-H., Wu, C.-H., Ladurner, A., Mizuguchi, G., Wei, D., Xiao, H., Luk, E., Ranjan, A. and Wu, C. (2009b). N terminus of Swr1 binds to histone H2AZ and provides a platform for subunit assembly in the chromatin remodeling complex. *J. Biol. Chem* **284**, 6200-6207.
Xing, S., Salinas, M., Höhmann, S., Berndtgen, R. and Huijser, P. (2010). miR156-targeted and nontargeted SBP-box transcription factors act in concert to secure male fertility in *Arabidopsis*. *Plant Cell* **22**, 3935-3950.
Xu, Y., Ayrapetov, M. K., Xu, C., Gursoy-Yuzugullu, O., Hu, Y. and Price, B. D. (2012). Histone H2A.Z controls a critical chromatin remodeling step required for DNA double-strand break repair. *Mol. Cell* **48**, 723-733.
Xu, M., Hu, T., Smith, M. R. and Poethig, R. S. (2016a). Epigenetic regulation of vegetative phase change in *Arabidopsis*. *Plant Cell* **28**, 28-41.
Xu, Y., Guo, C., Zhou, B., Li, C., Wang, H., Zheng, B., Ding, H., Zhu, Z., Peragine, A., Cui, Y. et al. (2016b). Regulation of vegetative phase change by SWI2/SNF2 chromatin remodeling ATPase BRAHMA. *Plant Physiol.* **172**, 2416-2428.
Yang, L., Xu, M., Koo, Y., He, J. and Poethig, R. S. (2013). Sugar promotes vegetative phase change in *Arabidopsis thaliana* by repressing the expression of *MIR156A* and *MIR156C*. *Elife* **2**, e00260.
Yang, H., Howard, M. and Dean, C. (2014). Antagonistic roles for H3K36me3 and H3K27me3 in the cold-induced epigenetic switch at *Arabidopsis* FLC. *Curr. Biol.* **24**, 1793-1797.
Yi, H., Sardesai, N., Fujinuma, T., Chan, C. W., Veena, and Gelvin, S. B. (2006). Constitutive expression exposes functional redundancy between the *Arabidopsis* histone H2A gene *HTA1* and other *H2A* gene family members. *Plant Cell* **18**, 1575-1589.
Yu, S., Cao, L., Zhou, C.-M., Zhang, T.-Q., Lian, H., Sun, Y., Wu, J., Huang, J., Wang, G. and Wang, J.-W. (2013). Sugar is an endogenous cue for juvenile-to-adult phase transition in plants. *Elife* **2**, e00269.
Yu, N., Niu, Q.-W., Ng, K.-H. and Chua, N.-H. (2015). The role of miR156/SPLs modules in *Arabidopsis* lateral root development. *Plant J.* **83**, 673-685.
Yun, J. Y., Tamada, Y., Kang, Y. E. and Amasino, R. M. (2012). *Arabidopsis* trithorax-related3/SET domain GROUP2 is required for the winter-annual habit of *Arabidopsis thaliana*. *Plant Cell Physiol.* **53**, 834-846.
Zhang, T.-Q., Lian, H., Tang, H., Dolezal, K., Zhou, C.-M., Yu, S., Chen, J.-H., Chen, Q., Liu, H., Ljung, K. et al. (2015). An intrinsic microRNA timer regulates progressive decline in shoot regenerative capacity in plants. *Plant Cell* **27**, 349-360.